Feghhi et al. Journal of Theoretical and Applied Physics 2014, 8:1
http://www.jtaphys.com/content/8/1/1

Journal of Theoretical and Applied Physics
a SpringerOpen Journal

RESEARCH Open Access

Investigation of the optimal material type and dimension for spallation targets using simulation methods

Seyed Amir Hossein Feghhi[1], Zohreh Gholamzadeh[2*] and Claudio Tenreiro[2,3]

Abstract

Accelerator-driven systems are extensively developed to generate neutron sources for research, industrial, and medical plans. Different heavy elements are utilized as spallation targets to produce spallation neutrons. Computational methods are efficiently utilized to simulate neutronic behavior of a spallation target. MCNPX 2.6.0 is used as a powerful code based on Monte Carlo stochastic techniques for spallation process computation. This code has the ability to transport different particles using different physical models.

In this paper, MCNPX has been utilized to calculate the leaked neutron yield from Pb, lead-bismuth eutectic (LBE), W, Ta, Hg, U, Th, Sn, and Cu cylindrical heavy targets. The effects of the target thickness and diameter on neutron yield value have been investigated via the thickness and diameter variations between 5 to 30 cm and 5 to 20 cm, respectively. Proton-induced radionuclide production into the targets as well as leaked neutron spectra from the targets has been calculated for the targets of an optimum determined dimension. The 1-GeV proton particle has been selected to induce spallation process inside the targets. The 2-mm spatial FWHM distribution has been considered for the 1-mA proton beam.

Uranium target produced the highest leaked neutron yield with a 1.32 to 3.7 factor which overweighs the others. A dimension of 15 × 60 cm is suggested for all the cylindrical studied spallation targets. Th target experienced the highest alpha emitter radionuclide production while lighter elements such as Cu and Sn bore the lowest radiotoxicity. LBE liquid spallation target competes with the investigated solid targets in neutronic point of view while has surpass than volatile liquid Hg target.

Keywords: Simulation; Spallation neutron yield; Radionuclide production; MCNPX 2.6.0 code

PACS: 28.65. + a; 28.41.Ak; 29.25.-t

Introduction

Neutrons are uncharged and interact with nuclei rather than atomic electrons. The scattering cross-section varies randomly throughout the periodic table and between various isotopes. This fact allows an effective discern of light atoms in the presence of heavier ones, to distinguish between neighboring elements and to exploit isotopic substitution (contrast variation) to isolate or highlight particular features or components. The energies of thermal neutrons are similar to those of atomic and molecular dynamics, enabling motions from polymer reptation to molecular vibrations and lattice modes to be probed. The neutron magnetic moment enables magnetic structure and fluctuations to be investigated. Neutrons are highly penetrating, enabling the use of complex sample environments. They are also non-destructive, allowing studies of delicate biological materials without damage. They perturb the material under study only weakly. This greatly aids theoretical interpretation, making analysis generally straightforward and direct [1]. X-ray is an electromagnetic radiation, and its scattering is a very effective probe in locating electron cloud and nuclei of high Z atoms in a sample.

Neutrons have also been widely utilized in imaging systems. Neutron scattering shows some advantages over previously mentioned X-ray scattering phenomena. Neutron is an effective tool in locating hydrogen atoms in a

* Correspondence: cadmium_109@yahoo.com
[2]Department of Physics, Talca University, Talca, Chile
Full list of author information is available at the end of the article

molecule due to the fact that neutron-proton scattering cross section is large. This is particularly important for the study of biological samples [2].

The most important procedures in producing neutron sources are fission reaction in reactors and spallation phenomena in accelerator-driven systems. Spallation neutron sources are of interest for transmutation of long-lived actinides and fission products from nuclear waste [3], plutonium from nuclear weapons [4], or thorium (as an energy source) [5], used for material research and industry [6] or medicine for radiotherapy [7].

The ranges of parameters for accelerator-driven systems meeting the three main applications of accelerator-driven systems are transmutation, industrial applications, and power generation. An accelerator beam power of 1 to 2 MW can be used for transmutation of reactor spent fuel, while the other applications demand higher beam powers mainly 10 to 75 MW [8].

For neutron spallation sources, the materials which closely qualify in a point of view of different criteria such as high thermal conductivity and stress resistance in front of high-energy proton irradiation are as follows: tin, tungsten, tantalum, and depleted uranium as solid targets and mercury, lead, lead-bismuth eutectic, and lead-gold eutectic as liquid targets [9].

In principle, since spallation reaction takes place in all elements by high-energy particle beam injection, all high-density heavy materials make suitable spallation targets. The number of released neutrons is proportional to the atomic number of the elements. In practice, however, there are a number of requirements, which limit the possible choices considerably.

The most important ones for solid targets are the following: good thermal conductivity at the temperature of operation, small thermal expansion coefficient to minimize thermal stress (in particular fatigue stress), good elastic properties and sufficient ductility even after irradiation, resistance to corrosion even under irradiation, low radiotoxicity, and reasonably good manufacturability and joinability to other materials (by welding, hipping, or other techniques) [10].

Computational codes are extensively being used to simulate accelerator-driven systems (ADS). Among them, MCNPX™ is a general purpose Monte Carlo radiation transport code designed to track many particle types over broad ranges of energies. It is the next generation in the series of Monte Carlo transport codes that began at Los Alamos National Laboratory nearly 60 years ago. MCNPX 2.6.0 includes many new capabilities, particularly in the areas of transmutation, burn-up, and delayed particle production. The code involves extension of neutron, proton, and photonuclear libraries to 150 MeV and the formulation of new variance reduction and data analysis techniques. The program also includes cross-sectional measurements, benchmark experiments, deterministic code development, and improvements in transmutation code and library tools through the CINDER90 project [11].

Hence, neutronic investigation of different heavy targets using MCNPX particle transport code to determine an optimum dimension and most favorable material as spallation target has been proposed in the present research.

Materials and methods

Different targets of ^{238}U, Th, Pb, lead-bismuth eutectic (LBE), Ta, W, Hg, Au-Pb, Cu, and Sn have been irradiated by proton beams of 1 GeV, respectively. A proton beam current of 1 mA (2-mm spatial FWHM) has been introduced on the upper surface of the targets. The projectile energy has been selected considering the fact that up to 1 GeV the neutron yield enhancement is approximately a linear function of the energy and for higher energies the yield falls off from the linear correlation because of the production and non-productive decay of π0 particles into pairs of 70-MeV photons [12]. Although lower energies can be applied, the selected energy is the upper limit which can obtain maximum neutron yield.

To determine the optimal thickness, the length of the cylindrical target (5 cm in diameter) has been varied to 5, 10, 15, 20, 25, and 30 cm, respectively. Then, the target diameter has been changed to 5, 10, 15, and 20 cm in a constant length value, respectively. Some neutronic parameters such as the leaked neutron yield and the heat deposition have been calculated for targets in different diameters and thicknesses, respectively. An optimum dimension has been suggested for the targets using the achieved neutronic data and proton range calculations in the targets using stopping and range of ions in matter (SRIM) code and another formula [13,14]. Residual nuclei and neutron spectra have been calculated for the optimized dimension targets. F6 tally has been used to calculate heat deposition in the spallation targets, and F1 tally has been used to calculate neutron spectra.

Determination of neutron spectra

To determine neutron spectra in a surface, F1 tally can be employed. Each time a particle crosses the specified surface, its weight is added to the tally, and the sum of the weights is reported as the F1 tally in the MCNP output. When problem geometry is voided (zero density), the tally is useful for verifying conservation of energy and conservation of number of particles. Technically, if $J(r, E, \Omega) \equiv \Omega\Phi(r, E, \boldsymbol{\Omega})$ were the energy and angular distribution of the flow (current vector) as a function of position, the F1 tallies would measure

$$F_1 = \int_A dA \int_E dE \int_{4\pi} d\Omega n \cdot J(r_s, E, \Omega), \quad (1)$$

where n is the outward normal to the surface at r_s [15].

Determination of heat deposition

In the energy range, where nuclear data tables are available, the neutron, photon, and proton energy deposition is determined using the heating numbers from the nuclear data tables. These heating numbers are estimates of the energy deposited per unit track length. In addition, the dE/dx ionization contribution for electrons and/or protons is added in for MODE E or MODE H.

Above the tabular energy limits, or when no tabular data is available, energy deposition is determined by summing different factors. For charged particles, ionization (dE/dx) energy is deposited uniformly along the track length (which is an important factor, when creating mesh tallies). All other energy deposition is calculated at the time of a nuclear interaction. The energies of secondary particles, if they are not to be tracked (i.e., not included on the MODE card) will be deposited at the point of the interaction. Nuclear recoil energy will be deposited at the point of interaction, unless heavy ion transport is specified. In order to obtain the most accurate energy deposition tallies, the user must include all potential secondary particles on the MODE card. PEDEP card can be used to calculate energy deposition [11]. The tally scores the energy deposition using Equation 2 [16]:

$$F_6 = \frac{\rho_a}{\rho_g}\int_v\int_t\int_E H(E)\Phi(r,E,t)dEdt\frac{dV}{V}\left(\frac{\text{MeV}}{\text{g} * (\text{Source particle})}\right), \tag{2}$$

where ρ_a is the atom density (atoms/barn cm), ρ_g is the gram density (g/cm^3), and $H(E)$ is the heating response (summed over nuclides in a material). F6 tally for neutrons is calculated via

$$H(E) = \sigma_T(E)H_{ave}(E), \tag{3}$$

in which

$$H_{ave}(E) = E - \sum\nolimits_i P_i(E)\left[\bar{E}_{out}(E) - Q_i + \bar{E}_{\gamma i}(E)\right] \tag{4}$$

and σ_T is the total neutron cross section, E is incident neutron energy, $P_i(E)$ is the probability of reaction i, E_{out} is the average exiting neutron energy for reaction i, Q_i is the Q value of reaction i, and $\bar{E}_{\gamma i}$ is the average energy of exiting gammas for reaction i.

F6 tally for photons is calculated via the following equation that the heating number is

$$H(E) = \sigma_T(E)H_{ave}(E) \tag{5}$$

$$H_{ave}(E) = \sum\nolimits_{i=1}^{3} P_i(E) * (E - \bar{E}_{out}) \tag{6}$$

$i = 1$ incoherent (Compton) scattering with form factors, $i = 2$ pair production, and $i = 3$ photoelectric [16]. F6 tally has been used to calculate heat deposition into the targets.

Residual nuclei tally

Histp card has been used to calculate radionuclide production in any spallation targets. Histp card presence in input computational program can produce residual output file after each run in which the output file is readable using HTAPE3X execute file. Residual masses have been transferred to picogram (pg) scale by multiplying the N^{HTAPE} data with A (mass number) × 1.036402E – 08 (g) [17]. Large history of particles has been used to reduce the calculation errors to less than 0.5%. INCL4/ABLA model has been used for residual nuclei calculations. Gas production into the targets has been considered using IOPT 8 card. The other carried out calculations has been obtained using the MCNPX default physical model, Bertini/Drenser.

Different possible spallation targets

Tungsten is one of the materials which present chemically inert, low corrosion (gas coolant), resistance to radiation damage (approximately 1 year), good availability, and low price that are close to that of an ideal spallation target. In other words, tungsten is one of the targets that can provide the most spallation neutron. Although the absorption of neutrons is an undesirable property of tungsten, it can be outweighed by its high neutron yield [18]. However, tungsten was found to corrode with water under irradiation, which is why Ta cladding is used [10]. Thermal-induced stresses may affect mechanical stability of tungsten and thus require cladding. If the tungsten begins to break apart due to thermal fatigue, then radioactive solid particulates will be released in the coolant gas stream. Therefore, both steady state and transient (thermal cycling) stresses should be investigated for tungsten target [19].

Due to difficulties in the fabrication of the tungsten target and foreseen mechanical constraints (large stresses due to the concentrated energy deposition), it is more convenient to use tantalum instead of tungsten. Tantalum offers better machining and mechanical properties and similar neutronic characteristics with tungsten, although it is considerably more expensive [20]. In fact, some tantalum usage disadvantages make its choice more cautiously than tungsten based on the fact that W gives the highest neutron leakage per unit area and unit beam power due to its low resonant absorption. Relative to tantalum, there is about a 20% gain. At the same time, tungsten afterheat and radioactivity are significantly lower than for tantalum [21].

Molten lead (melting point 327°C) is a potential material for a liquid spallation target design. Its high neutron yield makes some advantage in point of view of its usage as a preferable spallation target material. Lead and LBE targets are quite similar in their overall performance, while LBE target has lower melting temperature (123°C) and good thermal/mechanical properties. When

the proton beam bombards LBE, a significant amount of heat will be deposited within the target, and keeping it in a liquid phase seems easier than the other liquid targets. Preventing the target from boiling (1,665°C) is another advantage of LBE [22].

Unfortunately, Pb-Bi is potentially corrosive and produces polonium as by-product of spallation, but the eutectic alloy lead-bismuth was successfully applied in the MEGAPIE spallation target at SINQ at the Paul Scherer Institute [23].

Accelerator-driven test facility (ADTF) center used LBE as spallation target. According to this report, the target surface temperature of the structural material in contact with the LBE was limited to less than 550°C to avoid any corrosion problem. This temperature limit was assumed based on the fact that the coolant chemical structure was closely controlled to maintain an oxide layer on the structural surface for corrosion protection. The coolant inlet temperature should be set up to 200°C, which provides adequate design margin above the LBE melting point of 129°C. The LBE should maintain oxygen concentration in the range of 10^{-4} to 10^{-6} at.% to avoid corrosion problems [24].

As a part of the ESS Preparatory Phase Project in the University of Latvia, the possibility of using the Pb-17% Au eutectic (melting point 212°C) for the ESS target has been considered. In general, a molten Pb-Au eutectic alloy can successfully replace mercury within a liquid target, but the solid tungsten may provide a moderately higher thermal neutron flux [23]. A liquid mercury target for the MW-scale target is also being developed because of its advantages of self-circulating heat removal and neutron yield.

In JSNS, mercury was selected as a target material for neutron generation in consideration of its neutron generation efficiency and the cooling process [25]. Interaction of energetic proton beam with mercury target leads to high heating rates in the target, while its boiling point is 357.53°C. Temperature rise is enormous during a brief beam pulse of 0.7 μs which will be in the order of 10^7°C/s repeated at 60-Hz frequency. Consequently, thermal shock-induced compression of mercury leads to production of large amplitude high-frequency pressure waves in mercury that interacts with mercury target container [26].

Prior to that, JSNS utilized a solid metal target typically made of tungsten, but the required tenfold increase in performance which was required from JSNS demanded an improved technology. The technical team decided to employ a liquid mercury target which created significant technical challenges in materials engineering and heat transfer. The use of a liquid metal target also requires safety concerns about the possibility of a release of radiation in the event of an accident. In the JSNS report, it has been demonstrated that there are many tasks and concerns to be cared on the safety side to make sure that there would not be any kind of public health or safety risks [27].

There are many problems in using fissile materials as a fuel in spallation neutron sources. Major problems are swelling, growth inside the fissile material, and delayed neutron production, which contribute as a constant time-independent background in the output flux of neutrons. These problems could be reduced or eliminated using a non-fissile element in the target. Tungsten and tantalum are the attractive materials that could replace uranium in spallation neutron sources due to their very good and well-known characteristics beside their high neutron production per incidence [28]. A uranium solid target could be used, up to a proton beam power level of about 1 MW. However at 5 MW, the above time-integrated current could be reached only in 3 weeks. Neglecting the radiation-induced damages, the use of a liquid metal target would be more practical than a solid target. Service lives of U target systems were much shorter than expected; in the worst case at ISIS, the shortest life was reported to be approximately only 1 month. In the case of U targets, the end of the service life was considered to be when an appreciable, sometimes a detectable, amount of fission products appeared in the primary cooling water or in its cover gas. Therefore, it is believed that the use of a U target using the proton beam power at present ISIS, 160 kW, would be very difficult and impractical. Thus, the use of a non-actinide target becomes a unique solution at a higher power level [29].

The heavy metal spallation targets become 'hot cell' materials after a long period of irradiation. The radioactivity is due to the spallation residuals produced through reactions with various primary and secondary particles. The estimation of these products is very important due to production of some alpha-emitting (^{146}Sm, ^{148}Gd, ^{150}Gd, ^{154}Dy, ^{210}Po, etc.) toxic elements in heavy metal targets.

Irradiation of light targets such as Sn will produce beta emitters with relatively short half-lives. The estimation of the radio-activity/toxicity is an important parameter to select the spallation/coolant material. The other advantage of tin is that heat as well as neutron distribution is more spread over tin target volume compared to LBE. The neutron yield is 15% to 30% lower for the tin isotopes compared to that from Pb and/or LBE [30].

Copper has low n/p yield, low atomic number ($z = 29$), low density (8.933 g cm^{-3}), high thermal conductivity (385 W m^{-1} K^{-1}), and high melting point (1,084.62°C) [31]. Radiation laboratory of California University used copper as target material in 1951 and studied nuclear reactions induced in copper which was irradiated with charged particles, accelerated to energies of 340 MeV [32].

In the present research, an investigation and comparison of different neutronic parameters of various spallation targets have been reviewed.

Results and discussion

Leaked neutron yielded from the spallation target has been calculated for different target materials using MCNPX code. The results showed that the highest yield is obtainable using 238-U target. The second target which concludes in high neutron yield is W. Then, Pb, LBE, and Au-Pb targets result in identical neutron yields. Ta and Hg targets have exceeded than the Pb group in this parameter, while there is not much difference between Th and Ta targets specially in thinner thicknesses of the target. Lighter elements such as Cu and Sn produce the least neutron yields than the others. For most of the targets, after 25-cm thickness, there is not much growth in neutron yield, and the relative growth occurred in a factor less than 5%, while Pb group and Sn targets have a noticeable growth mainly 7% to 9% after 25 cm (Figure 1).

Hence, a 30-cm target thickness has been chosen, and the target diameter has been changed from 5 to 20 cm. Computational data demonstrated that the increment of diameter increases the leaked neutron yield noticeably up to 15-cm diameter for all the investigated targets. After 15-cm diameter, a maximum of 3% relative growth will occur in leaked neutron yield (Figure 2).

It is considerable that Th and W curves overlap each other thoroughly, which means thorium spallation target behaves similarly to tungsten target in neutronic yield, using these dimensions (Figure 2).

To choose an optimum target, other factors such as heat deposition should be considered. As it could be seen in Figure 3, the highest heat deposition occurs for 238-U target. The other targets bear noticeably less heat than uranium target, which is descending by the target length enhancement. Also, the heat deposition per centimeter for all the irradiated targets is closing to each other by increasing the target length.

Energetic protons and nuclei interact with matter mostly by collisions with electrons. These lead to progressive energy loss.

Bethe's formula does not allow obtaining an analytic expression of the projectile range. A common approximation, which allows reasonable proton range estimates, is the following:

$$R_{\mathrm{el}} = \frac{205A}{\rho Z} \ (\mathrm{cm}), \tag{7}$$

where A, Z, ρ are the mass number, the charge, and the mass density of the target nucleus, respectively [14].

The range of 1-GeV protons is calculated by SRIM code and other formula and is approximately less than 60 cm; hence, they should be completely absorbed in 60-cm-long targets (Table 1). Although proton range is less than 60 cm in heavier targets such as ^{238}U, due to neutronic parameters' comparison in identical dimension for all spallation targets, this length value has been selected for all of them. The 60-cm height is suggested

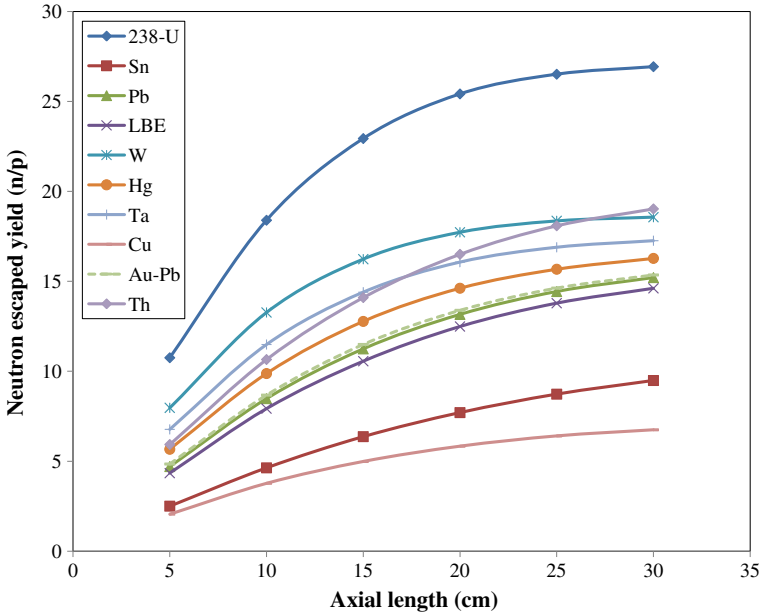

Figure 1 Comparison of leaked neutron yield variations in effect of target thickness enhancement. Target diameter = 5 cm.

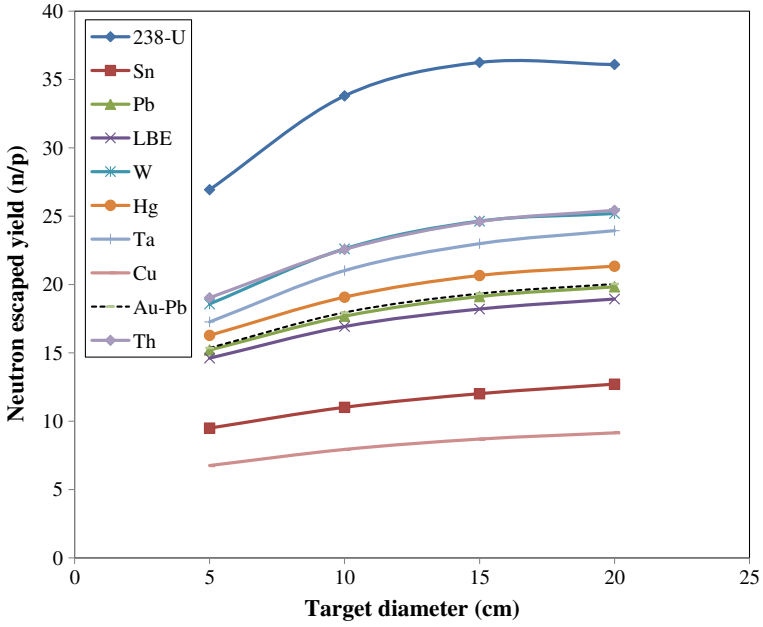

Figure 2 Comparison of neutron yield variations in effect of target diameter enhancement. Target thickness = 30 cm.

to provide complete interaction of 1-GeV protons with the spallation target material before escaping from the spallation target. A 15 × 60 cm cylindrical dimension is suggested for the spallation targets in both neutron yield and thermal hydraulic point of views.

As Table 1 denotes, 1-GeV proton injection in a 15 × 60 cm cylindrical target results in the highest heat deposition in uranium target with a value of 26 MeV/cm. The other investigated targets experience approximately closed heat depositions in the order of 8.08 to 9.5 MeV/cm. The leaked neutron yield of Pb group, W, Ta, and Hg is in the range of 21.1 to 24.8, the most leaked neutron yields belong to ^{238}U and Th targets, 36.8 and 27.7, respectively, and the least leaked neutrons produce by means of Sn and Cu targets, 15 and 9.74, respectively. Hg and U targets have the weakest thermal conductivity

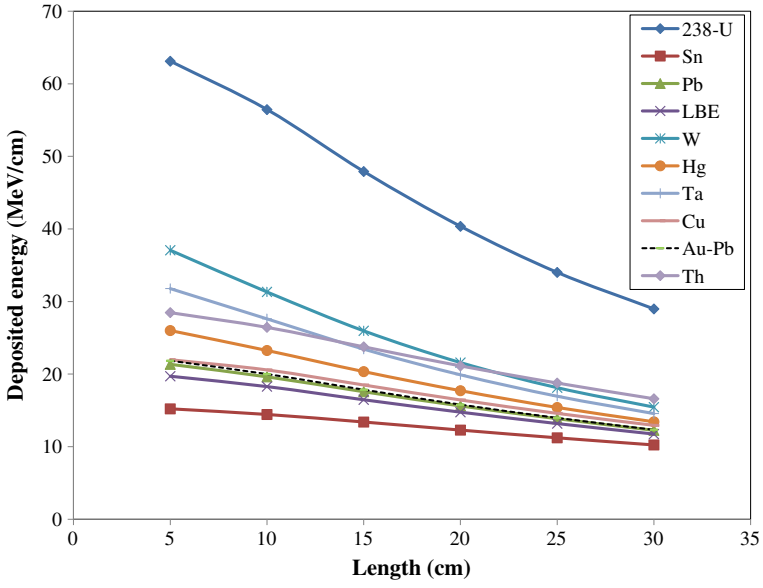

Figure 3 Comparison of energy deposition variations in effect of target length enhancement. Target diameter = 5 cm.

Table 1 Physical and neutronic properties of the different spallation targets, 15-cm diameter, 60-cm length

Number	Element	HD (MeV/cm)	Yield (n/p)	Calculation error (%)	MP (°C)	BP (°C)	Density (g/cm^3)	TC (W m^{-1} K^{-1})	PR (SRIM) (cm)	PR [13] (cm)
1	Au-Pb	8.76	21.6	0.58	418.0	1937	12.21	89.40	47.933	42.46
2	Pb	8.74	21.5	0.59	327.46	1749	11.35	35.00	53.741	45.85
3	LBE	8.64	21.1	0.60	123.0	1665	10.52	22.85	57.289	49.10
4	W	9.50	24.8	0.57	3422	5555	19.30	173.0	30.705	26.38
5	Th	13.3	27.7	0.61	1750	4788	11.72	54.00	53.886	45.08
6	Ta	9.31	23.5	0.58	3017	5458	16.40	57.00	35.878	30.98
7	Hg	9.07	22.0	0.59	−38.83	356.7	13.53	8.300	44.828	37.98
8	Sn	9.42	15.0	0.68	231.9	2602	7.287	67.00	73.160	62.98
9	Cu	8.08	9.74	0.65	1084	2562	8.933	385.0	53.204	50.64
10	U	26.0	36.8	0.59	1135	4131	19.10	27.00	33.228	27.76

HD, heat deposition; MP, melting point; BP, boiling point; TC, thermal conductivity; PR, proton range.

coefficients (8.3 and 27 W m^{-1} K^{-1}, respectively), while Cu and W targets benefit the highest values (385 and 173 W m^{-1} K^{-1}, respectively).

As Table 1 shows, the calculation uncertainties were less than 0.6% in average. As another result obtained in Table 1, it should be mentioned however that Th and W behaved similarly for escaped neutron yield using 30-cm spallation target thickness and different radii (Figure 2) but escaped neutron yield from Th target surpasses than W using 15 × 60 cm dimension clearly because of its longer stopping power for 1-GeV protons. U spallation target can achieve higher neutron yield in comparison with the other spallation targets with a factor of 1.32 to 3.7.

Other factor for selection of an optimal spallation target is its minimum radiotoxicity after irradiation. Hence, radionuclide production has been calculated for all the spallation targets. According to the obtained data, Th target experiences the most alpha emitter radionuclide production ($A > 210$) after irradiation. Among the other studied targets, uranium has the second score in this case. Pb, Au-Pb, and LBE have approximately identical behaviors in all mass numbers, and high mass number radionuclide production ($150 < A < 180$) is noticeably less in them than Ta and W. Hg radionuclide production curve is approximately close to the Pb groups, while up $A < 143$, its values are underestimated than Pb groups and after $A > 143$ are overestimated. Ta and W behave identically in all mass number range, and their curves are more underestimated than Hg, Pb, Au-Pb, and LBE curves up to 134 mass number, while after the mass number, there is a noticeably overweighing in radionuclide production mass into Ta and W targets. Au-Pb target experiences less radionuclide production than Pb and LBE targets up a mass number of 144, while after this, the Au-Pb data are overestimated than both of

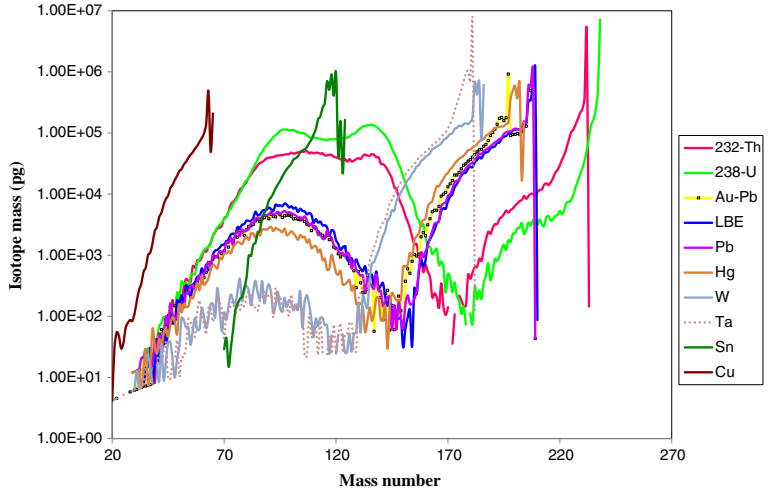

Figure 4 Comparison of radionuclide production in different spallation targets. Target diameter = 15 cm, length = 60 cm.

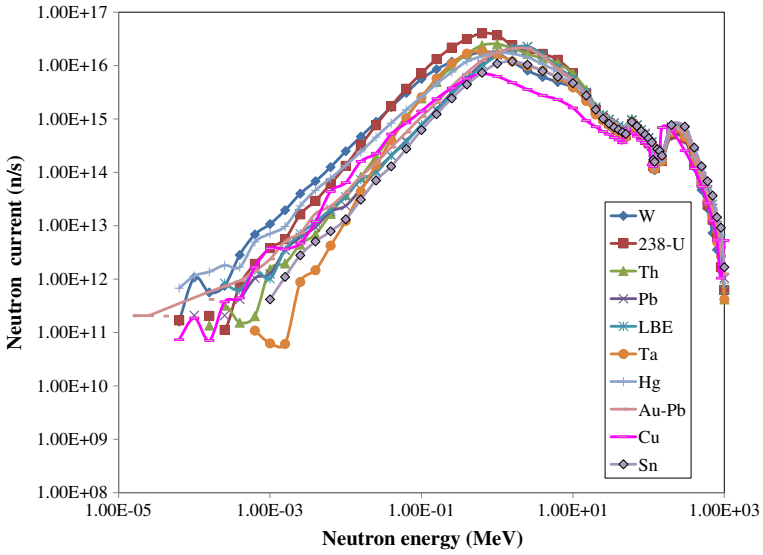

Figure 5 Comparison of leaked neutron spectra of different spallation targets. Target diameter = 15 cm, length = 60 cm.

them. Sn target produces more radionuclides in mass number range of 88 to 120 than Hg, Pb, Au-Pb, LBE, Ta, and W targets. Cu target produces more radionuclides in mass number range of 20 to 60 than Hg, Pb, LBE, Au-Pb, Th, U, Ta, and W targets. Whereas long-lived alpha emitter isotopes (americium-241, californium-252, polonium-210, plutonium-236, plutonium-239, radium-226, radon-222, thorium-220, thorium-229, thorium-232, and uranium-238) are produced in high mass number ranges, radiotoxicity of lighter targets such as Cu and Sn is clearly less than the others (Figure 4).

Neutron spectra have been calculated for the studied spallation targets. According to Figure 5, there are not noticeable relative discrepancies between the neutron spectra leaked from LBE, Pb, and Au-Pb spallation targets. Also, Ta and W neutron spectra were close to each other, but W target produces softer spectra than Ta. All the spallation targets had hard neutron spectra with 9.997% of $E_n > 1$ keV, except W and Cu. Fractions of escaped hard neutron spectra of W and Cu targets are 99.990% and 99.994%, respectively (Figure 5).

According to the data obtained in Figure 5, neutron spectra peak of U, W, and Ta targets are below 1 MeV (about 0.63 MeV), the LBE, Pb, Cu, and Au-Pb peaks are above 1 MeV (about 2.5 MeV), Hg and Sn have peaks about 1.58 MeV, and Th neutron spectra peak was at 1 MeV.

Gas production is another important factor which should be considered in target swelling point of view due to long time proton irradiations. Figure 6 shows that

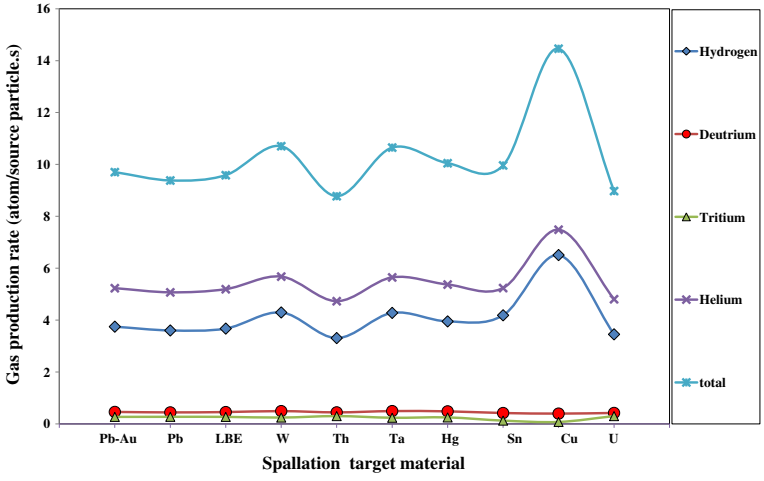

Figure 6 Comparison of gas production rate in different spallation targets. Target diameter = 15 cm, length = 60 cm.

Table 2 MCNPX (INCL4/ABLA) and AECL data comparison for neutron yield, proton energy: 960 MeV

Target material	Dimension (diameter × height) (cm)	MCNPX	Calculation error (%)	AECL experimental [37-40]	Relative discrepancy (%)
^{238}U	61 × 10.2	33.118	0.62	40.50	18.22
^{nat}Pb	61 × 20.4	21.776	0.59	20.46	−6.43
^{nat}Pb	61 × 10.2	17.910	0.64	16.46	−8.80
Sn	61 × 10.2	11.471	0.71	12.50	8.23
Be	91.6 × 10.2	2.445	1.18	2.70	9.44

Cu, W, and Ta experience the most hydrogen, deuterium, tritium, and helium gas production. Th and U targets experience the least gas production rate via 1-GeV proton induction into the target. Among the studied targets, Pb group experience less gas production than Sn and Hg targets.

Overall, fissionable elements seem not to be practical for ADS. Solid targets are less interesting in the point of view of thermal hydraulics, especially in high beam powers. Between the liquid targets, LBE presents more desirable parameters regarding both physical and neutronic properties. Au-Pb can be regarded as one of the best spallation targets with less radionuclide production than the others during 1-GeV proton irradiation, but its application demands more research in chemical resistance, thermal hydraulics, and economic performances.

The ACEL center carried out the experimental tests using different targets of 10.2-cm radius and 6-cm height irradiated by 0.96-GeV protons. These data are in good conformity with the simulation data obtained in the present research. Comparison between the experimental data for ^{nat}Pb of 20.4×61 cm^2 dimension and the present research (15×60 cm, 1 GeV) shows about 0.24% relative discrepancy [33].

Comparison of experimental and computational neutron yield for different targets irradiated by different incident energies

To evaluate confidence degree of computational and experimental data, a comparison between experimental neutron yield reported by AECL, BNL, and theoretical data obtained by MCNPX 2.6.0 code calculations has been carried out for different targets.

Table 3 MCNPX (INCL4/ABLA) and BNL data comparison for neutron yield, Pb target dimension: 10.2 × 61 cm

Energy (GeV)	MCNPX	Calculation error (%)	Experimental [41]	Relative discrepancy (%)
0.8	14.733	0.70	13.5	−9.13
1.0	18.695	0.63	17.5	−6.82
1.2	21.933	0.59	22.3	1.64
1.4	24.698	0.57	26.3	6.09

According to the literatures, INCL4/ABLA model can obtain more confidence data with experimental data [34-36]. In this work, the average relative discrepancy between experimental and theoretical using INCL4/ABLA model for neutron yield calculations was 7.24% (Tables 2,3,4).

According to the ACEL report, the experimental results obtained by the foil activation method are believed to be accurate to within ±5%. The computational obtained data in this work had an average uncertainty less than 0.7%.

A comparison between the experimental neutron yield achieved from Pb irradiation using 885-MeV proton energy and simulation using the INCL4/ABLA showed that the simulation data of 15.37 n/p is well matched with experimental 14.8 with about 3.85% relative discrepancy ([42]; see Additional file 1).

Conclusion

MCNPX stochastic code can be used to effectively evaluate the neutronic behavior of different spallation targets. Liquid targets can present more desirable performance circumstances especially using high beam powers, while their neutronic properties can efficiently compete with solid targets such as tungsten. An optimized 15-cm diameter and 60-cm height seem to achieve a desirable neutron yield leakage from the spallation targets irradiated by 1-GeV proton current. However, uranium target produced the highest leaked neutron yield with a factor of 1.32 to 3.7 higher than the others, but its application is limited because of its short operational half-life according to the reviewed literatures. Among the different liquid spallation targets, LBE offers more acceptable neutronic and physical properties while it will not suffer Hg vitality problems and high radionuclide impurity production.

Table 4 MCNPX (INCL4/ABLA) and BNL data comparison for neutron yield, W target dimension: 10.2 × 40 cm

Energy (GeV)	MCNPX	Calculation error (%)	Experimental [41]	Relative discrepancy (%)
0.8	14.895	0.68	15.0	0.70
1.0	19.102	0.59	20.5	6.81
1.4	27.193	0.53	28.5	4.58

Additional file

Additional file 1: Systematic studies of neutrons produced in the Pb/U assembly irradiated by relativistic protons and deuterons. Neutron production on lead target and its dependency on target sizes have been investigated in [42]. Simulations (MCNPX 2.6.C) of integral neutron production on the lead target ($R = 5$ cm, $L = 100$ cm) has been investigated. Dependency of integral neutron number on beam energy has been investigated in the present work. Some comparisons with the available experimental data have been carried out in this work.

Competing interests
The authors declare that they have no competing interests.

Authors' contributions
SAHF provided scientific support to the manuscript subject and data analysis. ZG carried out the simulations, designed the study, and drafted the manuscript. CT provided data analysis and computational support. All authors read and approved the final manuscript.

Acknowledgements
The authors gratefully acknowledge the cooperation of Talca University, Chile. This research was partially supported and funded by the university.

Author details
[1]Department of Radiation Application, Shahid Beheshti University, G.C, Tehran, Iran. [2]Department of Physics, Talca University, Talca, Chile. [3]Department of Energy Science, Sungkyunkwan University, 300 Cheoncheon-dong, Suwon, Korea.

Received: 5 April 2013 Accepted: 17 December 2013
Published: 6 January 2014

References
1. Cho, Y: Spallation Neutron Source. www.akpa.org/article/ycho.pdf (2008). Accessed 20 Feb 2008
2. Cho, Y: Synchrotron Based Spallation Neutron Source Concepts. NTIS, Alexandria (1998)
3. Bowman, CD, Arthur, ED, Lisowski, PW, Lawrence, GP, Jensen, RJ, Anderson, JL, Blind, B, Cappiello, M, Davidson, JW, England, TR, Engel, LN, Haight, RC, Hughes, HG, Ireland, JR, Krakowski, RA, LaBauve, RJ, Letellier, BC, Perry, RT, Russell, GJ, Staudhammer, KP, Versamis, G, Wilson, W: Nuclear energy generation and waste transmutation using an accelerator-driven intense thermal neutron source. Nucl. Inst. and Meth. in Phys. Res. A **320**, 336–367 (1992)
4. Lawrence, G: Transmutation and Energy Production with High Power Accelerators. IEEE, Piscataway (2006)
5. Carminati, F, Klapisch, R, Revol, JP, Roche, CH, Rubio, JA, Rubbia, C: An energy amplifier for cleaner and inexhaustible nuclear energy production driven by a particle beam accelerator. (1993). CERN report, CERN/AT/93-47(ET)
6. Mason, TE, Gabriel, TA, Crawford, RK, Herwig, KW, Klose, F, Ankner, JF: 33rd ICFA advanced beam dynamics workshop on high intensity and high brightness hadron beams, p. 21. AIP Conference Proceedings, Bensheim (2004)
7. Angelone, M, Atzeni, S, Rollet, S: Conceptual study of a compact accelerator driven neutron source for radionuclide production, boron neutron capture therapy and fast neutron therapy. Nucl. Inst. Meth. Phys. Res. **487**, 585–594 (2002)
8. Aït Abderrahim, H, Galambos, J, Gohar, Y, Henderson, S, Lawrence, G, McManamy, T, Mueller, AC, Nagaitsev, S, Nolen, J, Pitcher, E, Rimmer, R, Sheffield, R, Todosow, M: Accelerator and Target Technology for Accelerator Driven Transmutation and Energy Production. (2010). FERMILAB-FN-0907-DI, LA-UR-10-06754
9. Carpenter, JM: Pulsed spallation neutron sources for slow neutron scattering. Nucl. Inst. and Meth. **145**(1), 91–113 (1977)
10. Bauer, GS: Overview on spallation target design concepts and related materials issues. J. Nucl. Mat. **398**, 19–27 (2010)
11. Pelowitz, DB: MCNPX 2.6.0 manual, LANL, LA-CP-07-1473. Los Alamos National Laboratory, Los Alamos (2008)
12. Carpenter, JM, Gabriel, TA, Iverson, EB, Jerng, DW: The 10-GeV question: what is the best energy to drive a pulsed spallation neutron source. Physica B **270**, 272–279 (1999)
13. Ziegler, JF, Ziegler, MD, Biersack, JP: SRIM manual part A. IBM Research, New York (2006)
14. Nifenecker, H, Meplan, O, David, S: Accelerator Driven Subcritical Reactors (ADSR), p. 196. Institute of Physics, France (2002)
15. Shultis, JK, Faw, RE: An MCNP primer. Los Alamos National Laboratory, Los Alamos (2011)
16. Briesmeister, JF: MCNP - A General Monte Carlo N-Particle Transport Code Version4C. Los Alamos National Laboratory Report. Los Alamos National Laboratory, Los Alamos (2000). LA-13709-M
17. Broeders, I, Broeders, CHM: Neutron Physics Calculations for ADS Targets, p. 67. Institut f ¨ur Kern- und Energietechnik, Forschungszentrum Karlsruhe GmbH, Karlsruhe (2000)
18. Broome, TA: High power targets for spallation sources, p. 267. 5th European Particle Accelerator Conference, Barcelona (1996)
19. Ammerman, C, Woloshun, K, He, X, James, M, Li, N, Tcharnotskaia, V, Wender, S: Conceptual designs for a spallation neutron target constructed of helium-cooled, packed bed of tungsten particles. ANS Winter Meeting, Los Alamos National Laboratory (2001)
20. ENEA: The International TRADE Collaboration, 2nd TRADE Progress Report, ENEA Report. (2003)
21. Bauer, GS: Physics and technology of spallation neutron sources. Nucl. Inst. and Meth. in Phys. Res. A **463**, 505 (2001)
22. Gregson, MW: Full core analyze of ATW prototype for development of data for critical core components. MSc thesis, p. 14. The University of Texas at Austin (2003)
23. Cywinski, R, Bungau, C, Bungau, A: Target optimization studies for the European spallation source. MOPEA078, p. 256. Proceedings of IPAC'10, Kyoto (2010)
24. Gohar, Y, Herceg, J, Krajtl, L, Pointer, D, Saiveau, J, Sofu, T, Hanson, A, Todosow, M, Koploy, M, Mijatovic, P: Lead-Bismuth-Eutectic Spallation Neutron Source for Nuclear Transmuter. PHYSOR 2002, International Conference on the New Frontiers of Nuclear Technology: Reactor Physics, Safety and High-Performance Computing, Seoul (2002)
25. Kasugai, Y, Ooi, M, Kai, T: Gamma dose measurements and spectroscopy analysis for spallation products in JSNS mercury circulation system. Prog. Nucl. Sci. Technol. **1**, 501–504 (2011)
26. Mansur, LK, Gabriel, TA, Haines, JR, Lousteau, DC: R&D for the spallation neutron source mercury target. J. Nucl. Mat **296**, 1–16 (2001)
27. SNS: The Spallation Neutron Source Project. science.energy.gov/~/media/opa/pdf/SNS_033110.pdf
28. Improving the performance of a non-fissile target for spallation neutron sources. www.iasj.net/iasj?func=fulltext&aId=45852
29. Watanabe, N: Material Issues for Spallation Target by GeV Proton Irradiation Center for Neutron Science. Japan Atomic Energy Research Institute, Ibaraki-ken (1998)
30. Kumawat, H, Kailas, S: Spallation reaction with tin isotopes. Bhabha Atomic Research Centre, India, ADS/ND-07. International Topical Meeting on Nuclear Research Applications and Utilization of Accelerators, Vienna (2009)
31. Thermal Conductivity for all the elements in the Periodic Table. periodictable.com/Properties/A/ThermalConductivity.html
32. Batzel, RE, Miller, DR, Seaborg, GT: The high energy spallation products of copper. Phys. Rev **84**(4), 671–683 (1951)
33. Steinberg, M: Accelerator spallation reactors for breeding of fissile fuel and transmuting fission products. Brookhaven National Laboratory, Department of Nuclear Energy, Upton (1981)
34. Leray, S: HINDAS High-Energy Programme: main conclusions and implications for spallation neutron sources. Proceedings of the International Workshop on Nuclear Data for the Transmutation of Nuclear Waste, GSI-Darmstadt (2003). ISBN 3-00-012276-1
35. Rousseau, P: Validation of Calculation Tools for the Estimation of Reaction Products in the Target of Accelerator Driven Systems, p. 34. Institut für Reaktorsicherheit, Forschungszentrum Karlsruhe GmbH, Karlsruhe (2004)
36. David, JC, Boudard, A, Fernández-Dominguez, B, Leray, S, Volant, C: Fission within the spallation process. Influence of interanuclear cascade and evaporation modelizations on the fission fragment production. XVIth International Workshop on Physics of Nuclear Fission, Obninsk (2003)
37. Carpenter, JM: Neutron production, moderation, and characterization of sources. 1–23. www.neutron.anl.gov/NeutronProduction.pdf (2004). Accessed 16 Aug 2004

38. Johnson, JO, Gabriel, TA, Bartine, DE: Accelerator breeder nuclear fuel production concept evaluation of a modified design for ORNL'S proposed TMF-ENFP. Engineering Physics and Mathematics Division, Oak Ridge National Laboratory, Oak Ridge (1986). ORNL/TM—8999
39. Maiorino, JR, Mongelli, ST, Dos Santos, A, Anefalos, S, Deppman, A, Carluccio, T: A review of models and codes for neutron source (spallation) calculation for ADS application. International Nuclear Conference – INAC, Santos (2005)
40. Zucker, MS, Tsoupas, N, Vanier, PE, von Wimmersperg, U, Mughabghab, SF, Schmidt, E: In: Tsoupas, N (ed.) Relativistic Heavy Ion Collider. Brookhaven National Laboratory, Upton (1996)
41. Kumar, V, Kumawat, H, Goel, U, Barashenkov, VS: Neutron spallation source and Dubna cascade code. Pramana J. Phys. **60**(3), 469–481 (2003)
42. Wagner, V: Systematic studies of neutrons produced in the Pb/U assembly irradiated by relativistic protons and deuterons. NEMEA-4 Workshop, Prague (2007)

doi:10.1186/2251-7235-8-1
Cite this article as: Feghhi *et al.*: **Investigation of the optimal material type and dimension for spallation targets using simulation methods.** *Journal of Theoretical and Applied Physics* 2014 **8**:1.